01 Jan 1975

Strain Effects On The ESR Spectrum From Antimony Donors In Germanium

Edward Boyd Hale
Missouri University of Science and Technology, ehale@mst.edu

John R. Dennis

Shih Hua Pan

Recommended Citation

E. B. Hale et al., "Strain Effects On The ESR Spectrum From Antimony Donors In Germanium," *Physical Review B*, vol. 12, no. 7, pp. 2553 - 2561, American Physical Society, Jan 1975.
The definitive version is available at https://doi.org/10.1103/PhysRevB.12.2553

Strain effects on the ESR spectrum from antimony donors in germanium*

Edward B. Hale, John R. Dennis, and Shih-Hua Pan†
Department of Physics and Graduate Center for Materials Research, University of Missouri-Rolla, Rolla, Missouri 65401
(Received 27 March 1975)

The electron-spin-resonance spectra from surface-strained (but not externally stressed) antimony-doped germanium are investigated in detail. Experimental data are given for the linewidth, line asymmetry, and line-shape reversal feature as well as for the changes in donor concentration, temperature, and surface conditions. The donors of interest occur in a surface layer several microns thick. A theoretical analysis is based on the Kohn-Luttinger formulation for a shallow donor electron, which is forced by surface strain to predominately occupy a [111] conduction-band valley minimum. A substantial distribution in strain among the donor sites is necessary to account for the line-structure features. These features are predicted by a distribution function, which is calculated by using a narrowed Lorentzian line for a homogeneous line shape and a Gaussian strain distribution that determines the inhomogeneous broadening caused by strain-induced g-value variations. The one order of magnitude increase in linewidth with angle is attributed primarily to a $g^{-3}(\theta)$ dependence of the linewidth on strain. The asymmetry shape ratio of about 3 is attributed primarily to variations in the valley-population probabilities at different donor sites. The line-shape reversal feature is caused by an angular-dependent variation in the change of the g value with valley-population coefficients. For detailed calculations, distributed strain along the predominately occupied valley axis is assumed. It is found that the average compressive strain along the [111] axis is 10^{-4} with an accuracy of about 40% and that the Gaussian strain width is 0.6×10^{-4}. This average strain corresponds to a predominant valley occupation of 99%. Our analysis can be used as a semiquantitative tool for determining strain conditions in Ge(Sb).

I. INTRODUCTION

The electron-spin-resonance spectra from antimony donors in germanium depends somewhat on the ingot, but is usually a broad, anisotropic donor line[1,2] and/or a particular four-line spectrum,[3-6] sometimes called the "new" resonance. This paper reports experimental and theoretical results about the new resonance. Of basic interest are the data on linewidth, line asymmetry, and the associated line-shape reversal feature. Some results on donor dependence, temperature dependence, and surface conditions are also reported. In addition, calculations are presented which can account for the data. From these calculations, information is obtained on the strain and its distribution over the donors in a surface layer which is several microns thick. Also discussed is why the antimony spectrum is different from that of other shallow donors.

The signals of interest were originally reported by Pontinen and Sanders.[4] Later, these investigators associated the signals with the surface[3]—an important point apparently not realized by several subsequent investigators.[5,6] The spectrum has a g tensor which is characteristic of a donor electron in a single conduction-band valley. Different strains cause different valleys to be occupied, and hence a four-line spectrum is observed. The theoretical analysis of Keyes and Price,[7] which introduced the Kohn and Luttinger formalism[8] for donor impurities, was used to interpret the observations. They suggested that internal strains caused the single-valley rather than the multi-valley character of the electron. Our present calculations have extended the Keyes and Price model in a quantitative way. This extension has enabled us to characterize the nature of the strains at the donors and to understand the unusual linewidth, line asymmetry, and shape reversal features in the spectra.

II. EXPERIMENTAL DETAILS

A. Apparatus

The ESR measurements were made with a rotating Varian 12-in. magnet with Fieldial control and a Varian X-band spectrometer, which included a homemade, cylindrical copper cavity. Signals were normally recorded in the absorption phase at high (~100 mW) microwave power levels. The modulation field was 200 Hz and was applied by coils external to the Dewar. Most measurements were made at 4.2 °K, although some samples were studied down to 1.2 °K. The sample and cavity were totally immersed in a liquid-helium bath. On critical runs, the amplitude of the modulation was carefully controlled to avoid line-shape distortion.

A DPPH (diphenyl picryl hydrazyl) calibration sample was placed in the cavity. It was used to measure the relative amplitude changes in the Ge(Sb) signals and also to verify that the spectrometer was working in absorption.

B. Samples

The dimensions of the samples were approximately 2 cm × ½ cm × ½ mm. The samples were cut in our laboratory from wafers or ingots obtained from external sources, which included Purdue University, Semi-Metals, Western Electric, General Diode, and Eagle Picher Industries. Normally, the [1̄10] axis was along the magnet rotation axis. Some samples were studied which had different growth axes. Samples were also prepared so that they had different crystal axes normal to a damaged surface. The samples were etched, and their two large surfaces were damaged by sandblasting. Signals from several dozen different samples from six different ingots were investigated.

III. EXPERIMENTAL RESULTS

A. General observations

Signals were obtained from samples grown by either Semi-Metals or Purdue University. Signals were seen in samples with donor concentrations as high as $5\times10^{16}/\text{cm}^3$ and as low as $2\times10^{15}/\text{cm}^3$. Signals were found only in those samples that had damaged, not etched, surfaces. Figure 1 shows a plot of the magnetic field at resonance obtained

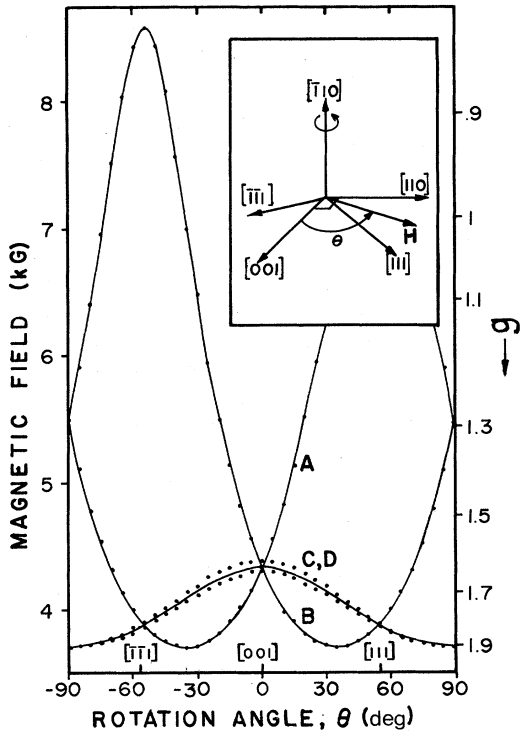

FIG. 1. ESR spectra from the surface-strained antimony donors in germanium at a microwave frequency of 9.94 GHz with $T=4.2$ °K and $N_d=0.8\times10^{16}/\text{cm}^3$.

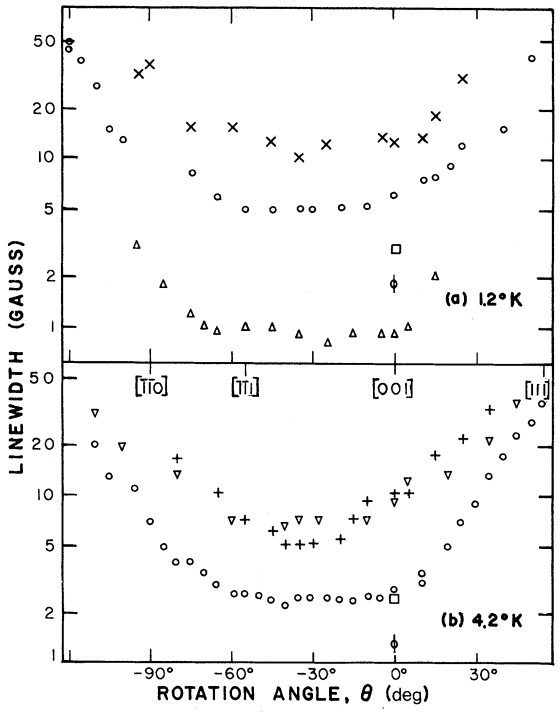

FIG. 2. Linewidth dependence on angle at different temperatures and donor concentrations for line A. The linewidth was measured as the peak-to-peak field separation of the recorded line shape. Symbols for our data are: $N_d=10^{16}/\text{cm}^3$ (×), $2.5\times10^{16}/\text{cm}^3$ (○), $0.2\times10^{16}/\text{cm}^3$ (▽), and $0.8\times10^{16}/\text{cm}^3$ (+). Symbols for Ge(Sb) subjected to a large external stress of 1.7×10^9 dyn/cm^2 as given in Ref. 10 are: $N_d=3\times10^{16}/\text{cm}^3$ (□), $5\times10^{16}/\text{cm}^3$ (φ), $7\times10^{16}/\text{cm}^3$ (△). [The Ref. 10 data in (a) are actually at 1.4 °K, but extrapolation suggests it would be nearly the same at 1.2 °K.]

from a typical sample as a function of the angle θ measured from the [001] axis in the (110) plane. The solid lines are calculated for an electron spin of ½ with a ⟨111⟩ axially symmetric g tensor whose components are

$$g_{\parallel}=0.828\pm0.003 \quad \text{and} \quad g_{\perp}=1.915\pm0.001. \qquad (1)$$

These values are in excellent agreement with the values of Pontinen and Sanders[3]. The spectral lines are designated by the letters A, B, C, and D and are derived from electrons, which are specifically associated with each of the four different ⟨111⟩ k-space valleys. In particular, line A is associated with the [111] valley. [For perfect crystal alignment (<0.1°), lines C and D would be degenerate.] Significantly lower signal intensities at high magnetic fields make data taking more difficult for low g values. Data for $g<1.1$ are reported for the first time. More detailed line structure results are discussed below.

B. Linewidth results

The linewidths and intensities change substantially with changes in the magnetic field. An increasing linewidth corresponds to decreasing intensity as expected for an unchanging spin concentration. Figure 2 shows the more than one order of magnitude change in linewidth of line A as a function of the angle θ. (All linewidths measured and discussed refer to the peak-to-peak separation of the first derivative of the absorption curve.) Figure 2 also shows that changes with donor concentration and temperature have been observed.

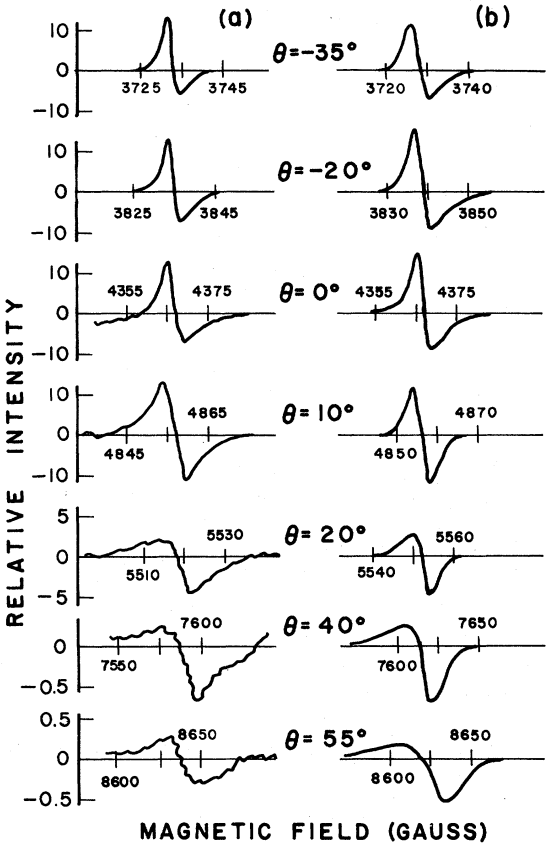

FIG. 3. Angular dependence of the line-shape features. (a) Contains data from a typical sample at 4.2 °K with $N_d = 2.5 \times 10^{16}/\text{cm}^3$. (b) Contains the computed result from Eq. (12) for a model discussed in the text with $y_0 = -6$, $\delta y = 2$, and $\delta H = 2$ G. Both the x and y axes have been rescaled for the bottom three plots. Note the symmetrical shape at $\theta = 10°$, the asymmetrical shape at other angles, the inversion of shape for angular changes around 10°, and the substantial broadening and amplitude reduction at large θ. (The difference in the resonance fields between (a) and (b) at the same angle is within the experimental error limits.)

C. Line asymmetry results

The line shape also exhibits interesting asymmetric characteristics, which repeat under a variety of passage conditions and are attributed to the inherent line shape. Figure 3(a) shows how this feature varies with angle for line A. The asymmetric shape is clearly seen at $\theta = -35°$, but not at 10°. Figure 3(a) also shows the large variation of linewidth and intensity with angle.

D. Shape reversal results

The reversal and loss of the asymmetric shape is rather unusual. Figure 3(a) shows that this occurs for less than a 20° change in θ near 10°. Measurements show that this is not a passage effect. It was duplicated in numerous samples from various ingots and was not observed to have a donor concentration or temperature dependence.

E. Surface condition results

Some experiments were conducted to investigate the surface conditions necessary for observing the signals. Samples with damaged surfaces gave signals, whereas thoroughly etched samples did not. The surfaces were damaged either by roughing them with sandpaper or diamond-saw scratches or by sandblasting them with different grades of abrasive powder at various jet pressures. These various damage methods influenced the intensity of the lines, but had very little effect on the basic line structural features.

A gradual surface stripping experiment was performed with a dilute CP4 etch (HF: acetic acid: HNO_3: liquid bromine in the ratios 50:50:80:1). Etches of five minutes each were used to remove a surface layer of the sample. Between etches, measurements of the ESR signals were made relative to a DPPH standard signal. Sample thickness measurements were made with a micrometer. The basic structural features of the lines remained unchanged, and the lines decreased in intensity after each etch. This indicates the strain characteristics are essentially uniform throughout the surface layer and are hence more characteristic of bulk strains rather than of monolayer strain. The results of the experiment are shown in Figure 4. Essentially, the line intensities were reduced by a factor of 10 after 6 μm were stripped off.

F. Other results

The line asymmetry and reversal features were essentially unchanged for various donor concentrations and temperatures; however, the absolute and relative line intensities varied over a wide range depending on the sample. For example, we were

only able to find signals in the ingots obtained from Semi-Metals and Purdue University. Signals were not found in ingots provided by three other suppliers. It thus seems that original growth conditions influence the type of strain produced by the surface damage. It has been reported that[5] the growth axis influences the relative intensity of the lines. We were not able to find any systematic variation of line intensity with [111] or [110] growth-axis ingots. Also, no systematic variations were found in samples with [100], [112], [111], or [110] surface normals. The bulk sample dislocation density did not seem to be important as has been observed for other donors.[2] Further studies with controlled growth variables would be informative.

Annealing experiments in vacuum, air, and oxygen or nitrogen environments at temperatures up to 300 °C had no substantial effect on the signals. This condition indicated substantial chemical stability.

IV. MODEL AND ANALYSIS

A. Introduction

The Keyes and Price model[7] seems very plausible—the essence of the model being that the resonance is from a one-valley donor electron subjected to a large, [111] axis, compressive strain. This explains the observed g tensor. It was determined that the strain is a result of surface damage.[3] With these ideas as a foundation, a quantitative model has been developed which can account for the more detailed structural features. The model is a bulk model with the near surface region providing the strain. The standard Kohn and Luttinger formulation[8] for a shallow donor electron is used. The valley-orbit matrix approach[9] is introduced to account for the effects of the strain. The line structural features occur because the strain has a substantial distribution rather than a unique value.

B. g tensor

The g tensor for a shallow donor electron[8] is

$$\vec{\vec{g}} = \sum_{j=1}^{4} \alpha_j^2 \vec{\vec{g}}_j , \tag{2}$$

in which the sum is over the four valleys, α_j^2 is the valley occupation probability, and $\vec{\vec{g}}_j$ is the jth-valley g tensor. In the crystal axes frame, the one-valley g tensor for the [111] valley is

$$\vec{\vec{g}}_1 = \begin{pmatrix} g_0 & \Delta & \Delta \\ \Delta & g_0 & \Delta \\ \Delta & \Delta & g_0 \end{pmatrix}, \tag{3}$$

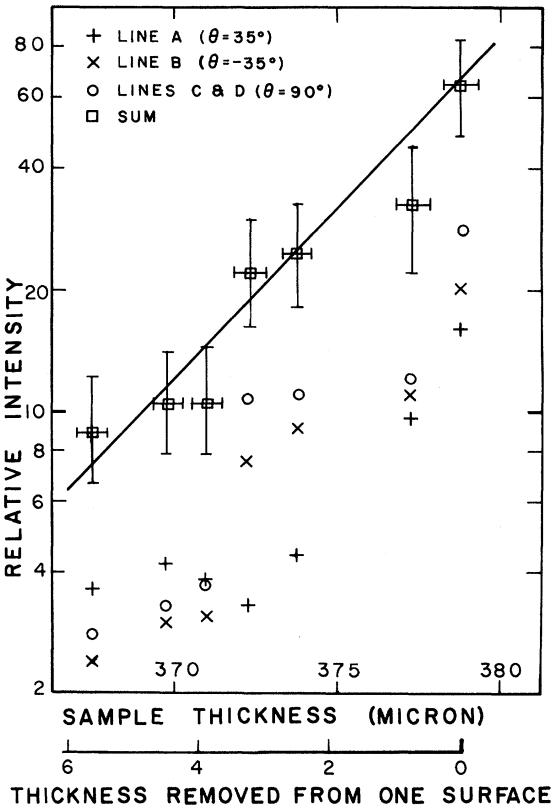

FIG. 4. Depth of strained donors as determined from a series of CP4 etches. The symbols are for line A at $\theta = 35°$ (+), for line B at $\theta = -35°$ (×), for lines C and D at $\theta = 90°$ (○), and for the composite sum (□).

in which g_0 and Δ are the two independent tensor components. The g tensors for the other valleys require appropriately symmetrized changes of sign in several of the off-diagonal elements. Calculations yield for the total tensor

$$\vec{\vec{g}} = g_0 \vec{\vec{1}} + \Delta \begin{pmatrix} 0 & \gamma_1 & \gamma_2 \\ \gamma_1 & 0 & \gamma_3 \\ \gamma_2 & \gamma_3 & 0 \end{pmatrix}, \tag{4}$$

in which the γ coefficients are the following combination of the valley population coefficients:

$$\begin{aligned} \gamma_1 &\equiv \alpha_1^2 - \alpha_2^2 - \alpha_3^2 + \alpha_4^2 , \\ \gamma_2 &\equiv \alpha_1^2 - \alpha_2^2 + \alpha_3^2 - \alpha_4^2 , \\ \gamma_3 &\equiv \alpha_1^2 + \alpha_2^2 - \alpha_3^2 - \alpha_4^2 . \end{aligned} \tag{5}$$

The measured g value can be expressed as

$$\begin{aligned} g(\theta) = \{ & g_0^2 + 2\Delta g_0 [\gamma_1 \sin^2\theta + \sqrt{2}\,(\gamma_2 + \gamma_3) \sin\theta \cos\theta]^{1/2} \\ & + \Delta^2 [\gamma_1^2 \sin^2\theta + (\gamma_2^2 + \gamma_3^2) \cos^2\theta + (\gamma_2 + \gamma_3)^2 \sin^2\theta \\ & + \sqrt{2}\,\gamma_1 (\gamma_2 + \gamma_3) \sin\theta \cos\theta]\}^{1/2} , \end{aligned} \tag{6}$$

in which θ describes the direction of the magnetic field as shown in Fig. 1.

Equation (6) can describe the spectra in Fig. 1 only if the electron is predominately in one valley, i.e., line A requires $\gamma_1 \approx \gamma_2 \approx \gamma_3 \approx 1$ so $\alpha_1 \approx 1$, $\alpha_2 \approx \alpha_3 \approx \alpha_4 \approx 0$. The only strain which produces a predominate one-valley population is a compressive $\langle 111 \rangle$ axis strain. Experiments have shown this predominate occupation through the application of a large $\langle 111 \rangle$ unaxial compressive stress[2,10]. (In such experiments, only a single line is observed. Here, four lines are seen because the surface damage does not discriminate between the four possible $\langle 111 \rangle$ strain axes.) When the strained valley-orbit Hamiltonian is used in Schrödinger's equation, the valley populations for an [111] axis strain are obtained as[2]

$$\alpha_1^2 = \tfrac{1}{4}[2 - (1+2y)/(1+y+y^2)^{1/2}] \tag{7a}$$

and

$$\alpha_2^2 = \alpha_3^2 = \alpha_4^2 = \tfrac{1}{3}(1 - \alpha_1^2)\,, \tag{7b}$$

with y, a convenient, dimensionless, strain parameter, given by

$$y \equiv 8\Xi_u s/9E_{13}\,, \tag{8}$$

in which s is the magnitude of the strain,[11] Ξ_u [= 19 eV (Ref. 13)] is the shear deformation potential at the conduction-band minima and E_{13} [$= 3.2 \times 10^{-4}$ eV (Ref. 14)] is the singlet-triplet energy splitting for the ground state. For the predominant valley population, y is negative because the donor is *compressively* strained. We thus refer to more negative y values as greater strains.

Equation (6) yields for line A

$$g(\theta) = [g_0^2 + 2\gamma^2\Delta^2 + \gamma\Delta(2g_0 + \gamma\Delta)(\sin^2\theta + 2\sqrt{2}\sin\theta\cos\theta)]^{1/2} \tag{9}$$

in which

$$\gamma \equiv \gamma_1 = \gamma_2 = \gamma_3 = \tfrac{1}{3}(4\alpha_1^2 - 1)\,. \tag{10}$$

The fit of Eq. (9) to the spectra in Fig. 1 yields

$$g_0 = \tfrac{1}{3}(g_\parallel + 2g_\perp) = 1.553 \pm 0.002 \tag{11a}$$

and

$$\gamma\Delta = \tfrac{1}{3}(g_\parallel - g_\perp) = -0.3623 \pm 0.002\,. \tag{11b}$$

C. Line structural features

1. Narrow line shape at large g values

The small linewidth at large g values and the absence of donor hyperfine lines suggest that line narrowing is important. The narrowing, which is probably due to exchange rather than motion,[15] has been observed for the other shallow donor impurities in the same concentration range.[2] Such data show that the linewidth decreases with either increasing temperature or increasing donor concentration. These two dependences are also observed in the present case as Fig. 2 shows. For a better comparison, the available linewidth data[10] on externally stressed Ge(Sb) in the concentration range 10^{15}–$10^{17}/\mathrm{cm}^3$ are also shown in Fig. 2. The surface strain and externally stressed data are compatible. We conclude that line narrowing strongly affects the linewidth at large g values, i.e., $\theta = -35° \pm 50°$ for line A. At other angles, strain effects substantially influence the line shape.

2. Broad line shape at small g values

Line-shape broadening due to strain occurs due to a distribution in strain at the various donors. This distribution causes a distribution in g values, which can cause an inhomogeneous linewidth which exceeds the homogeneous linewidth. We calculate the derivative of the line shape since it is experimentally recorded. We write for the observed spectral distribution function

$$\frac{dI(H,\theta)}{dH} = \int_{-\infty}^{\infty} L(H - H')P(H',\theta)\,dH'\,, \tag{12}$$

where $L(H - H')$ is the field derivative of the homogeneous line-shape function, and $P(H',\theta)$ is the distribution function for the number of donors which have a resonance field in a range between H' and $H' + dH'$ at angle θ. In the present case, the homogeneous function is assumed to be Lorentzian so that

$$L(H - H') \equiv -2(H - H')(\delta H)^2/[(H - H')^2 + (\delta H)^2]^2\,, \tag{13}$$

in which $\delta H = \delta H(N_d, T)$ is $\frac{1}{2}$ the linewidth and has an N_d and T dependence as Fig. 2 shows.

$P(H',\theta)$ is determined by the strain distribution within the crystal. We assume a Gaussian distribution of strain along the predominately occupied valley axis. Thus, the probability of having a strain y in a range dy is

$$P(y) = A' \exp\{-[(y - y_0)/\delta y]^2\}\,, \tag{14}$$

where y_0 is the average strain, δy is 0.613 times the Gaussian width at halfmaximum, and A' is a normalization factor. Equation (14) is convertible to a field distribution and yields for line A at constant θ and microwave frequency

$$P(H',\theta) = A'' \frac{\exp\{-[(y - y_0)/\delta y]^2\} g^3(\theta)(y^2 + y + 1)^{3/2}}{2\gamma\Delta + (g_0 + \gamma\Delta)(\sin^2\theta + 2\sqrt{2}\sin\theta\cos\theta)}\,, \tag{15}$$

where Eqs. (7), (8), and (9) have been used and $A'' = 2A'\mu_B/h\nu\Delta$ since $h\nu = g(\theta)\mu_B H'$.

The spectral distribution function of Eq. (12) has

been computed using Eqs. (13) and (15). Results of such calculations are shown in Fig. 3(b) for $y_0 = -6$, $\delta y = 2$, and $\delta H = 2$ G. These parameters are appropriate to a typical sample with $N_d = 2.5 \times 10^{16}/\text{cm}^3$ at $T = 4.2$ °K. The values for y_0 and δy are chosen for reasons discussed below. Near $\theta \simeq -35°$, $P(H', -35°)$ is sharply peaked in H' compared to $L(H - H')$. In such a case, the derivative of the Lorentzian is predicted by Eq. (12) and such a shape is observed. The value for δH was obtained from the width at $\theta = -35°$. With this choice of parameters, agreements with the actual data in Fig. 3(a) are quite reasonable. The large change in linewidth is reproduced. The symmetric shape near $\theta = 10°$ and the asymmetric shape at other angles are also reproduced. In addition, the shape reversal between $\theta = 0°$ and $\theta = 20°$ is quite apparent.

Near $\theta = 55 \pm 20°$, $P(H', \theta)$ is very broad and primarily determines the line shape as Fig. 5 shows at $\theta = 40°$. (At other angles the shape of the curve is very similar, but both axes must be rescaled.) The field distribution would be Gaussian if the denominator, $(y^2 + y + 1)^{3/2}$, and the g^3 factors in Eq. (15) did not depend on strain. Actually, the denominator and g^3 factors have only a slight strain dependence and basically effect $P(H', \theta)$ through their angular dependence. The skewed Gaussian distribution is due to the $(y^2 + y + 1)^{3/2}$ factor. Figure 5 shows how this factor enhances the half of the distribution corresponding to the greater strains, while the lower strain half is reduced. The effect is to cause $P_{\max}$ to be at a field $H'(y_m)$ which corresponds to a larger strain y_m than the central Gaussian value y_0.

The ESR line shape is also plotted in Fig. 5. It was computed exactly, but its shape is very similar to dP/dH. This occurs whenever $P(H', \theta)$ is very broad compared to $L(H - H')$. The strains larger than y_0 cause an enhanced half line, while the smaller strains cause a reduced half line. Because the axis crossing occurs very near the field at $P_{\max}$, rather than at $H(y_0)$, y_m does not correspond to the average strain in the crystal but to a somewhat greater strain. This is important when trying to infer y_0 from g-tensor measurements.

3. *Asymmetric line features*

Two asymmetric line features occur because H does not vary linearly with y. One asymmetrical influence distorts the amplitude of the line (see Fig. 5). This effect is due to variations in the valley population coefficients with strain.

Another asymmetrical effect acts to broaden the line. This occurs because the change in H per unit strain varies significantly with strain. The quantity of interest is

$$\frac{dH'}{dy} = \frac{A'[2\gamma\Delta + (g_0 + \gamma\Delta)(\sin^2\theta + 2\sqrt{2}\,\sin\theta\cos\theta)]}{A'' g^3(\theta)(y^2 + y + 1)^{3/2}}. \tag{16}$$

Thus, for equal strain increments the field axis will be "scaled" by a factor $(y^2 + y + 1)^{3/2}$ ($\simeq y^{-3}$ for large y values). Figure 6 shows how H' varies with strain and reveals a substantial nonlinearity in H' for $y \lesssim -2$. [Equation (16) is the negative slope of the curve.] For the smaller strains, the curve is steep and a very broad, reasonably symmetric ESR line is expected. For larger strains, even a very broad strain distribution can produce a narrow line. In addition, the slope nonlinearity means that the high-strain side of the ESR line will be narrower than the low-strain side. However, this asymmetric effect will only be large for a

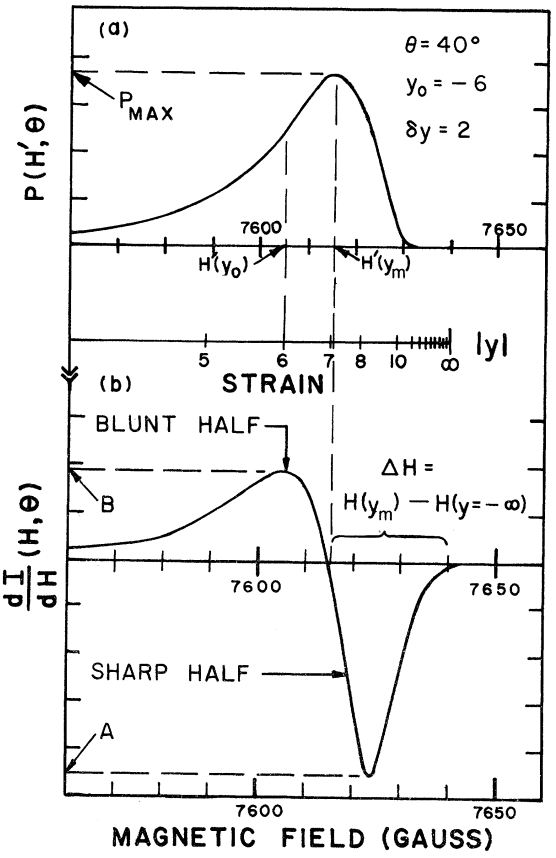

FIG. 5. Field dependence of both the inhomogeneous broadening function and derivative of the spectral distribution function. These line A calculations are at $\theta = 40°$ for a Gaussian strain distribution with an average strain $y_0 = -6$ and $\delta y = 2$. The peak of $P(H', \theta)$ is essentially at the axis crossing field of dI/dH and corresponds to a strain value y_m rather than y_0. For dI/dH, the peak-to-peak ratio A/B is a measure of the asymmetry. The base width of the sharp half-line ΔH can be estimated reasonably well from the experimental data.

large distribution in y values. In summary, the two asymmetric effects produce an enhanced, narrowed half-line, i.e., the sharply peaked half-line in Fig. 5 and a reduced, broadened half-line, i.e., the blunt half-line in Fig. 5.

The square-bracketed term and g^{-3} factors in both Eqs. (15) and (16) are weakly dependent on strain and are about the same for all parts of the line. However, they vary substantially with angle. They enhance or reduce the line amplitude, while at the same time they reduce or enhance the line spread. Thus, the shape of $P(H', \theta)$ is "rescaled" at each angle. For example, the g^3 factor is responsible for much of the change in line width and reduction in amplitude for the two angles $\theta = -35°$ and $\theta = 55°$ because $(g_\perp/g_\parallel)^3 = 12.4$.

4. *Shape reversal feature*

The shape reversal feature exists because the square-bracketed term in Eq. (16) changes sign with angle. Thus, the sign reversal angle θ_R must satisfy the equation

$$\sin\theta_R(\sin\theta_R + 2\sqrt{2}\cos\theta_R) = -2\gamma\Delta/(g_0 + \gamma\Delta). \tag{17}$$

For small strains, $\gamma \simeq 0$ and $\theta_R \simeq 0°$. For large strains, $\gamma \simeq 1$ and $\theta_R \simeq 11°$. For $y < -2$, θ_R is in the range $11° \pm 1°$. Hence, the reversal feature should occur over a small range near $\theta = 10°$.

The amplitude of $P(H', \theta)$ is reciprocally influenced by the square-bracketed term, whereas the width is linearly influenced. Thus, $P(H', \theta)$ becomes sharply peaked for angles near θ_R, and a nearly symmetric derivative of the narrowed Lorentzian is expected and observed.

Because both Eqs. (15) and (16) change sign at θ_R, a reversal in both the amplitude and field scaling is expected as θ varies through θ_R. This agrees with the observations at $\theta = 0°$ and 20° because Fig. 3 shows that both half-lines not only invert in magnitude, but also reflect about the axis crossing field.

D. Strain determination

1. *g tensor analysis*

The sensitivity of the line and line shape to strain reveals information on the strain and strain distribution in the crystal. The g tensor reveals that the strain is compressive and predominately along the ⟨111⟩ axis, otherwise Eq. (6) would not fit the data. The exact value of the strain cannot be directly determined because Eq. (9) shows that γ always occurs in a product with Δ. External stress measurements[2,3] can vary γ and have determined Δ as

$$\Delta = -0.36 \pm 0.01 . \tag{18}$$

This result, when combined with Eq. (11b), yields

$$\gamma = 1.00 \pm 0.03 . \tag{19}$$

This value corresponds to a predominate valley population of >97% and a strain $|y| > 3$. Figure 6 gives a nondetailed, pictorial idea of how this limit on y can be estimated from data at $\theta = 40°$. Because the ESR line was observed above 7500 G, the average strain value must lie beyond the major bend in the curve. Because the slope of the curve above the bend is small, only the lower strain limit near the bend can be determined.

To obtain the actual strain, a small correction must be made in the y_m value derived from the axis crossing field as previously discussed and shown in Fig. 5. This correction (estimated below to be about 15%) and Eq. (8) enable us to conclude that most of the observed surface donors are under a compressive [111] axis strain exceeding 10^{-4}.

2. *Line-shape analysis*

The line-shape data yields information on the strain distribution, which can be described by two parameters. First, the base width of the sharp half-line can be approximated from the data and is not difficult to estimate theoretically because $\Delta H = H(y_m) - H(y \to -\infty)$. The second parameter is

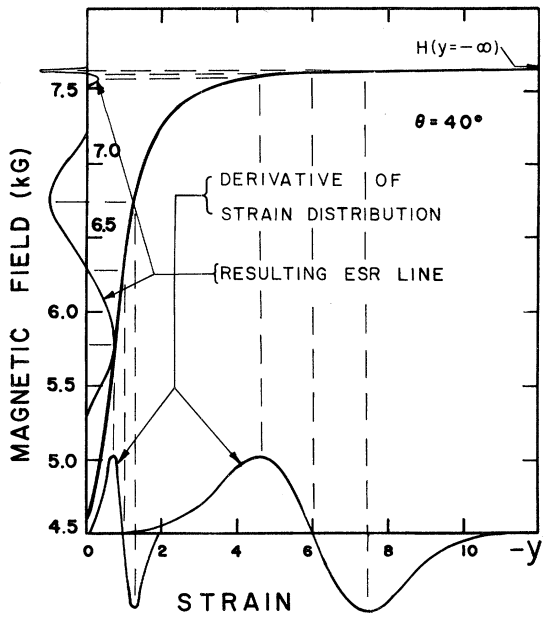

FIG. 6. Schematic method of obtaining line shape from strain distribution. A high field, narrow, asymmetric ESR line is expected only for a broad strain distribution with an average strain beyond the bend in the curve.

a measure of the asymmetry in terms of an A/B ratio, in which A is the amplitude of the sharp half-line and B is the amplitude of the blunt half-line as shown in Fig. 5. The above two parameters have been theoretically examined to see what best fits the data. A strain distribution with a small width will only produce a reasonably symmetric line. Hence, the asymmetry indicates that a broad strain distribution exists. At angles where $P(H', \theta)$ is broad, the A/B ratio varies from 2 to 5 depending on the crystal ingot. The most typical A/B ratio is 3. For the Gaussian distribution, such an A/B ratio corresponds to $\delta y/y_0 \approx \frac{1}{3}$. (For $\delta y/y_0 \approx \frac{2}{3}$, the A/B ratio is about 10.) For 40° and a $\delta y/y_0$ ratio of $\frac{1}{3}$, the sharp half-line base width, ΔH, is about 10, 15, 25, or 50 G depending on whether $y_0 = -10$, -8, -6, or -4, respectively, (The y_m values are about 15% higher in each case.) The data indicates $\Delta H \simeq 25$ G. We conclude that a Gaussian strain distribution with $y_0 = 6 \pm 2$ and a width at half-maximum equal to $1.6\delta y = 4 \pm 1$ can fit the data. This corresponds to a compressive strain of 10^{-4} with a Gaussian strain width of $\frac{2}{3}$ this value.

V. COMMENTS AND SUMMARY

The theory presented here should be valid not only for Ge(Sb) but for other shallow donor systems, whose surface ESR has not been reported. This lack of data is probably because equivalent strains s correspond to substantially different y values. For example, in Eq. (8), $E_{13}(\mathrm{P}) = 2.8 \times 10^{-3}$ eV,[14] and $E_{13}(\mathrm{As}) = 4.2 \times 10^{-3}$ eV,[14] hence $y_0(\mathrm{Sb}) = -6$ corresponds to $y_0(\mathrm{P}) = -0.7$ and $y_0(\mathrm{As}) = -0.45$. Figure 6 shows how these small y values would lead to an exceedingly broad and, hence, weak ESR line. However, near $\theta = \theta_R \simeq 5°$, the lines might just be observable.

Figure 6 is also helpful in understanding why the "normal" donor spectrum with hyperfine structure as seen in Ge(P) and Ge(As) is not observed in Ge(Sb). Wilson[2] found that typical deep bulk strains in doped germanium are $(3 \pm 2) \times 10^{-5}$. These strain values correspond to $y \simeq -2$ for antimony and hence to the substantial slope region of the curve. Thus, the line would be too broad and weak to observe even for a rather narrow strain distribution. However, for the other donors the smaller y values are such that the weak dependence of the reversal angle on strain makes observation of the resonance near $\theta \simeq 0°$ possible over a wide range of γ_1, γ_2, and γ_3 values. Observations vary from ingot to ingot,[2,5,16] but typically lines corresponding to the C and D valleys are seen over a wide range of θ, whereas the A and B valleys are seen only near $\theta = 0°$. This is because the g values for lines A and B change substantially with θ near 0°, which is not the case for the C and D lines.

Several assumptions in our model are too restrictive. One of these is that the Gaussian strain distribution is *only* along the predominant [111] strain direction. The data could be fit by other than a Gaussian distribution and, more importantly, by strain distributions along other directions. Calculations for directions, such as [001], [110], or other [111] axes, have been made. The calculations lead us to believe that the strain distribution must be broad, i.e., have a width which competes effectively with y_0 to change the valley population probabilities, the broadening should still be proportional to $g^{-3}(\theta)$, the shape reversal angle will still be near $\theta \simeq 10°$, and the asymmetric shape ratio could have a different, but still nonlinear character.

Another restrictive assumption concerns the fact that all angular dependence in the narrowed Lorentzian linewidth δH has been neglected. The increase in linewidth for $-10° < \theta < 20°$ is most likely due to a change of δH with angle. The fact that the donor concentration and temperature dependence exist over this rather large range in θ supports this idea. The theory of line narrowing[17] suggest that δH should vary as $[g(\theta)\nu_n(\theta)]^{-1}$, in which $\nu_n(\theta)$ is the average transition rate between states. Because the narrowing mechanism is not understood,[15] $\nu_n(\theta)$ is unknown. The inverse dependence on $g(\theta)$ increases the linewidth as observed, but not enough to completely account for the observations.

In summary, the Ge(Sb) surface resonance can be explained by a model originally suggested by Keyes and Price[7]. The model invoked uses the Kohn-Luttinger shallow donor model with the electron forced to predominately occupy a [111] valley by the damage induced [111] strain. Consideration of the spectrum yields a semiquantitative determination of the crystal strains at the donors. Our detailed analysis has shown that the linewidths, line asymmetry, and shape reversal features can all be understood by assuming a broad distribution in strain. The surface strains involved are about 10^{-4}.

---

*Research supported by the Air Force Office of Scientific Research and the National Science Foundation.

†Present address: Department of Physics, University of Utah, Salt Lake City, Utah 84112.

[1] G. Feher, D. K. Wilson, and E. A. Gere, Phys. Rev. Lett. 3, 25 (1959).

[2] D. K. Wilson, Phys. Rev. 134, A265 (1964).

[3] R. E. Pontinen and T. M. Sanders, Jr., Phys. Rev. 152,

850 (1966).
[4]R. E. Pontinen and T. M. Sanders, Jr., Phys. Rev. Lett. 5, 311 (1960).
[5]T. Mitsuma and K. Morigaki, J. Phys. Soc. Jpn. 20, 491 (1965).
[6]R. R. Hasiguti, T. Nakanishi, N. Funakoshi, and S. Takahashi, Radiat. Eff. 9, 57 (1971).
[7]R. W. Keyes and P. J. Price, Phys. Rev. Lett. 5, 473 (1960).
[8]W. Kohn, *Solid State Physics*, edited by F. Seitz and D. Turnbull (Academic, New York, 1957), Vol. 5.
[9]P. J. Price, Phys. Rev. 104, 1223 (1956).
[10]K. Morigaki and T. Mitsuma, J. Phys. Soc. Jpn. 20, 62 (1965).
[11]If s is the magnitude of the strain tensor, then the off-diagonal, "conventional" strain component (Ref. 12) for a [111] axis strain is $\frac{2}{3}s$.
[12]J. C. Hensel and G. Feher, Phys. Rev. 129, 1041 (1963), Appendix A.
[13]H. Fritzsche, Phys. Rev. 115, 336 (1959).
[14]J. H. Reuszer and P. Fisher, Phys. Rev. 135, A1125 (1964).
[15]D. L. Meier, W. F. Parks, and E. B. Hale, Phys. Rev. B 10, 814 (1974).
[16]R. E. Pontinen, Ph.D. thesis (University of Minnesota, 1962) (unpublished).
[17]P. W. Anderson, J. Phys. Soc. Jpn. 9, 316 (1954).